

# Direct generation of correlated four photons from spontaneous four-wave mixing

Yifan Li,<sup>1</sup> Justin Yu Xiang Peh,<sup>1</sup> Chang Hoong Chow,<sup>1</sup> Boon Long Ng,<sup>1</sup> Vindhya Prakash,<sup>1</sup> and Christian Kurtsiefer<sup>1,2</sup>

<sup>1</sup>Centre for Quantum Technologies, National University of Singapore, 3 Science Drive 2, Singapore 117543

<sup>2</sup>Department of Physics, National University of Singapore, 2 Science Drive 3, Singapore 117551\*

..... abstract to come here...

## I. INTRODUCITON

....

## II. EXPERIMENTAL SETUP

The SFWM process is driven by a weak cw pump (of frequency  $\omega_p$ ) detuned by  $\Delta_p$  from  $|5S_{1/2}, F = 1\rangle \rightarrow |5P_{3/2}, F = 2\rangle$  and a strong cw coupling field (of frequency  $\omega_c$ ) resonant to the  $|5S_{1/2}, F = 2\rangle \rightarrow |5P_{1/2}, F =$

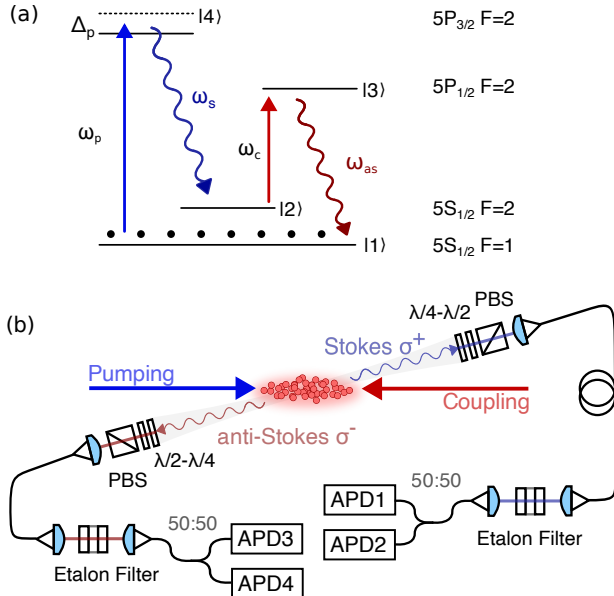


FIG. 1. (a) Energy levels involved in the Double- $\Lambda$  spontaneous four-wave mixing in <sup>87</sup>Rb. Solid blue and red arrows indicate cw pump and coupling fields respectively. Wiggly blue and red arrows indicate generated Stokes and anti-Stokes fields. Black dots indicate initialization of atoms in the  $F = 1$  hyperfine ground state. (b) Schematic of experimental setup. The pumping and coupling beams have a waist of  $\sim 0.85$  mm. The collection spatial mode is focused on the atomic ensemble with a waist of  $175$   $\mu$ m. Channels 1 and 2 analyze the Stokes field, and Channels 3 and 4 the anti-Stokes fields in a Hanbury-Brown-Twiss like setup.  $\lambda/2$ : Half waveplate,  $\lambda/4$ : quarter waveplate, PBS: polarising beamsplitter, Ch: channel, APD: avalanche photodiode.

$2\rangle$  transition. The Stokes photons are generated at a frequency  $\omega_s$  close to the  $|5P_{3/2}, F = 2\rangle \rightarrow |5S_{1/2}, F = 2\rangle$  transition and the anti-Stokes photons have a frequency  $\omega_{as}$  resonant to the  $|5P_{1/2}, F = 2\rangle \rightarrow |5S_{1/2}, F = 1\rangle$  transition (refer ??(a)). The fields are circularly polarized, orthogonal to each other, and are directed at an elongated magneto-optical trap (MOT) of cold <sup>87</sup>Rb atoms, along the long axis in a counter-propagating configuration ?? (b)). The atoms in the MOT are initialized in the  $|5S_{1/2}, F = 1\rangle$  hyperfine ground state and the MOT trapping beams are switched off during the SFWM measurement. The optical depth (OD) of the atomic cloud is  $\sim 30$ . The spatial modes for collection the Stokes and anti-Stokes photons are focused on the atomic ensemble with a waist of  $175$   $\mu$ m. The collection modes are at an angle of  $1^\circ$  to the pump and coupling fields, to reduce background scattering. Polarization filters and temperature controlled etalon filters (bandwidth  $\sim 100$  MHz) are implemented in both the Stokes and anti-Stokes collection arms to suppress unwanted photons. The photons collected in the Stokes and anti-Stokes arms are split using 50:50 fiber beamsplitters (BS) and detected using avalanche photodiodes (APDs). A timestamp card with 2 ns timing resolution records the photon arrival times in each of these four channels. Second, third and fourth-order field correlations are analyzed using this data.

## III. RESULTS

### A. Second-Order Correlation

We measure the second-order intensity correlations as a first step towards characterizing the statistical properties of the generated fields. The normalized second-order correlation between stationary fields  $\hat{E}_i$  in mode  $i$ , detected at time  $t_i$ , and  $\hat{E}_j$  detected at time  $t_j = t_i + \tau_{ji}$  is [? ]

$$g_{ji}^{(2)}(\tau_{ji}) = \frac{\langle \hat{E}_i^\dagger(t_i) \hat{E}_j^\dagger(t_i + \tau_{ji}) \hat{E}_j(t_i + \tau_{ji}) \hat{E}_i(t_i) \rangle}{\langle \hat{E}_j^\dagger(t_i + \tau_{ji}) \hat{E}_j(t_i + \tau_{ji}) \rangle \langle \hat{E}_i^\dagger(t_i) \hat{E}_i(t_i) \rangle}, \quad (1)$$

where  $i, j \in \{s, as\}$  for the Stokes ( $s$ ) and anti-Stokes ( $as$ ) mode.

The second-order autocorrelations  $g_{s,s}^{(2)}(\tau)$ ,  $g_{as,as}^{(2)}(\tau)$  and cross-correlation  $g_{s,as}^{(2)}(\tau)$  were measured for pump and coupling powers of about  $800$   $\mu$ W and  $10$  mW re-

\* christian.kurtsiefer@gmail.com

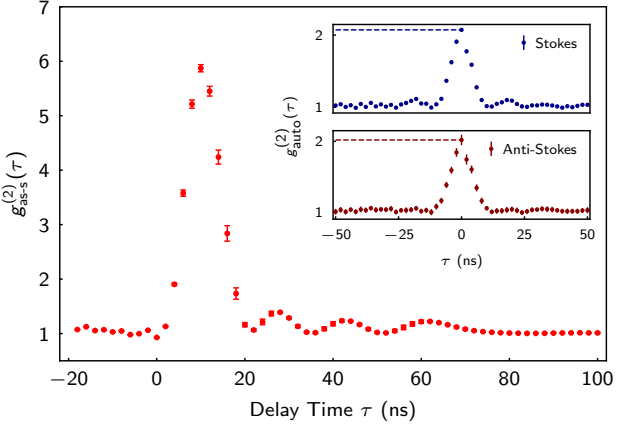


FIG. 2. Normalized second-order correlation. (a) The Stokes-anti-Stokes cross-correlation as a histogram of coincidences for various delays  $\tau$ , normalized by the Stokes and anti-Stokes singles rates for a 2 ns bin size and an integration time of 150 s. Results averaged over 17 measurements. Oscillations of periodicity 18 ns are caused by the Rabi frequency of the coupling field. Insets: Unheralded autocorrelation measurements of Stokes photons  $g_{s,s}^{(2)}(\tau)$  (blue) and anti-Stokes photons  $g_{as,as}^{(2)}(\tau)$  (red) (jointly labeled  $g_{\text{auto}}^{(2)}(\tau)$ ).

spectively and a pump detuning of  $\Delta_p = 40$  MHz. From the  $g_{s,as}^{(2)}(\tau)$  results shown in Fig.?? we infer a correlation time of around  $\Delta t = 16$  ns between the Stokes and anti-Stokes photons. The oscillations in the coincidences are due to the strong coupling beam which leads to an oscillation of population between energy levels  $|2\rangle$  and  $|3\rangle$  at an effective Rabi frequency of  $2\pi \times 55$  MHz[? ]. The pair generation rates inferred from these measurements are given in section ??.

The Stokes and anti-Stokes modes independently display thermal statistics as seen from their intensity autocorrelation at  $\tau = 0$  (inset in Fig.??). We measure  $g_{s,s}^{(2)}(0) = 2.07 \pm 0.02$  for the Stokes mode and  $g_{as,as}^{(2)}(0) = 2.02 \pm 0.07$  for the anti-Stokes mode.

## B. Triple Coincidences

We analyze the temporal distribution of coincidences involving more than two detections, to determine the ratio of correlated double-pairs to two independent pairs detected together by chance. Both these scenarios lead to states containing multiples of Stokes-anti-Stokes pairs and there is no physical mechanism that generates states involving three photons. Thus, a measurement of triplet coincidences involving two Stokes and one anti-Stokes photons or two anti-Stokes and one Stokes photon provides similar information to a four-fold coincidence measurement of two anti-Stokes and two Stokes photons, while being simpler to acquire and visualize.

The normalized third-order correlation between the

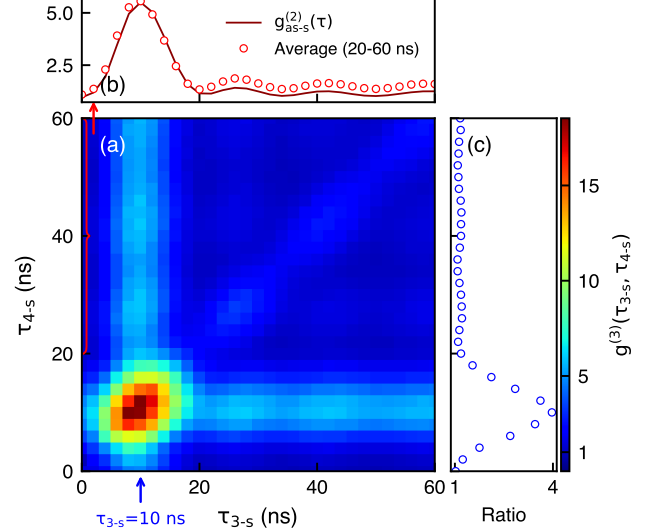


FIG. 3. Normalized third-order correlation. (a) Normalized triple coincidences  $g_{as,as,s}^{(3)}$  for various delays  $\tau_{3s}$  and  $\tau_{4s}$  between a detection in Ch3 and Ch4 respectively and a heralding Stokes photon in either of Ch1 or Ch2. Coincidences analyzed from data acquired over a measurement duration  $T_m$  of 0.7 h, normalized by the accidental triplet rate  $R_s R_3 R_4 \delta t^2 T_m$ , where the time bin  $\delta t = 2$  ns and  $R_i$  is the singles count in channel  $i$ . The  $g_{as,as,s}^{(3)}$  peak value of 18 indicates strongly correlated triplets. (b) Comparison of the vertical ridge with  $g_{as,s}^{(3)}$ . Red dots: Mean normalized triplet count, averaged over  $\tau_{4s}$  from 20 ns to 60 ns. Solid line: normalized cross-correlation function  $g_{as,s}^{(2)}(\tau_{3s})$  between Stokes and Ch3. (c) Ratio of normalized triple coincidence peak value with the average value along the vertical ridge away from the peak. Blue dots: Triple coincidences at  $\tau_{3s} = 8$  ns divided by mean triple coincidences at  $\tau_{3s} = 8$  ns and  $\tau_{4s} = 20 - 60$  ns. The peak is approximately 4 times the value in the ridge.

Stokes and anti-Stokes modes from two anti-Stokes detections at times  $t_3$  and  $t_4$  and a Stokes detection at time  $t_s$  is

$$g_{as,as,s}^{(3)}(t_3, t_4, t_s) = \frac{\langle \hat{E}_s^\dagger(t_s) \hat{E}_{as}^\dagger(t_3) \hat{E}_{as}^\dagger(t_4) \hat{E}_{as}(t_4) \hat{E}_{as}(t_3) \hat{E}_s(t_s) \rangle}{\langle \hat{E}_s^\dagger(t_s) \hat{E}_s(t_s) \rangle \langle \hat{E}_{as}(t_3) \hat{E}_{as}(t_3) \rangle \langle \hat{E}_{as}(t_4) \hat{E}_{as}(t_4) \rangle} \quad (2)$$

where the numerator gives the triple-coincidence rate  $G_{as,as,s}^{(3)}(t_3, t_4, t_s)$ . This can be expressed in terms of the second-order correlations as shown in the Appendix in Eq. ??.

Fig.?? shows  $g_{as,as,s}^{(3)}$  for triplets from an anti-Stokes detection each in channels 3 (at  $t_3$ ) and 4 (at  $t_4$ ) and a Stokes detection in either of channels 2 or 1 (at  $t_s$ ), where the measurement was performed for the same conditions as in section ?? . The results are represented in terms of relative delays  $\tau_{3s} = t_3 - t_s$  and  $\tau_{4s} = t_4 - t_s$ . The technique used to identify triplets from pair coincidences is described in the Appendix ??.

The features in Fig. ?? can be intuitively understood by analyzing Eq.?? over various delays. For a coherence time  $\Delta t$  for the Stokes and anti-Stokes photons, when  $\tau_{3s}, \tau_{4s}, \tau_{34} \gg \Delta t$ , the triplet rate reduces to the background accidental rate  $R^3(0)$  which is normalized to 1 here. When  $\tau_{3s}, \tau_{4s} \gg \Delta t$  and  $\tau_{34} \lesssim \Delta t$ , the autocorrelation in the anti-Stokes mode dominates the result  $(g_{as,as,s}(\tau_{3s}, \tau_{4s}, \tau_{34}) \rightarrow g_{as,as}^{(2)}(\tau_{34}))$ . In this case, the triplets are caused by the combination of an accidental click in the Stokes mode with a bunched thermal state in the anti-Stokes mode, forming the moderately bright diagonal in Fig. ??.

For  $\tau_{3s}, \tau_{34} \gg \Delta t$  but  $\tau_{4s} \lesssim \Delta t$  (horizontal ridge) or when  $\tau_{4s}, \tau_{34} \gg \Delta t$  but  $\tau_{3s} \lesssim \Delta t$  (vertical ridge) the cross-correlation between anti-Stokes (in Ch4 or Ch3) and Stokes photon-pairs are the dominant contributions. Here, the triplets are formed by a combination of a correlated Stokes-anti-Stokes pair with an uncorrelated photon in the other anti-Stokes channel. Thus, the maximum mean value in the horizontal and vertical ridges is equal to  $g_{as,as}^{(2)}(0)$  as seen in Fig. ?? (b).

In the region where  $\tau_{3s}, \tau_{34}, \tau_{4s} \lesssim \Delta t$  the coincidences increase several-fold. From Eq.??, using  $g_{as,as}^{(2)}(0) = 2$ , the theoretical peak value of the normalized triplet rate is  $g_{as,as,s}^{(3)}(0, 0, 0) = 4g_{as,s}^{(2)}(0) - 2 \approx 4g_{as,s}^{(2)}(0)$  when  $g_{as,s}^{(2)}(0) \gg 1$  which is true for highly non-classical pair sources. Thus, theoretically the peak is 4 times the maximum in either of the horizontal or vertical ridges when the output contains highly correlated four-photon states. When the output contains fewer correlated four-photons and more uncorrelated double-pairs from multiple SFWM events, the triplet peak at zero delays would arise from the overlapping of the ridges and would be closer to 2 times the maximum in either of the horizontal or vertical ridges.

Due to the long coherence time of the Stokes and anti-Stokes photons, our triplet measurement is not limited by averaging effects due to detector resolution, which would have otherwise reduced the maximum of the triplet-coincidence peak. We see from Fig. ?? (c) that in our measurement, the  $g_{as,as,s}^{(3)}$  peak is 18 and is about four times the mean along the vertical ridge (outside the central 20 ns window). Thus, we verify that the output of the SFWM process contains strongly correlated double-pairs, that contribute to the high three-fold coincidences in the triplet measurement.

### C. Quadrupole coincidences

We search for four-fold coincidences between detections of two photons in the anti-Stokes mode and two photons in the Stokes mode to obtain the double-pair generation rate and to directly verify the generation of correlated double-pairs from our SFWM source. The quadruplet rate for four-fold coincidences from two Stokes detections at times  $t_1$  and  $t_2$  respectively and two

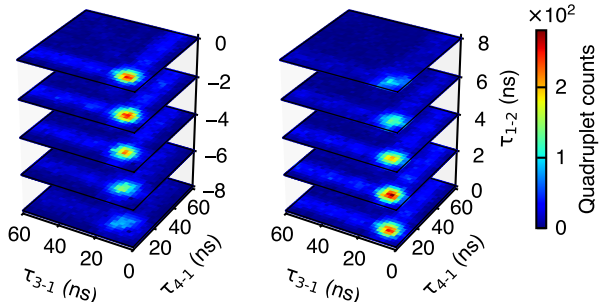


FIG. 4. Quadrupole-coincidence detection. Each slice shows unnormalized four-fold coincidences from a detection in each of Ch1 to Ch4 for a fixed delay  $\tau_{12}$  with a 2 ns time bin, and a range of delays  $\tau_{31}$  and  $\tau_{41}$ . Data acquired over a measurement duration of 0.7 hr. The coincidences are peaked for  $\tau_{12} = 0 \pm 2$  ns and  $\tau_{31}$  and  $\tau_{41} = 8 \pm 2$  ns.

anti-Stokes detections at time  $t_3$  and  $t_4$  respectively is described by the correlation function

$$G_{s,s,as,as}^{(4)}(t_1, t_2, t_3, t_4) = \langle \hat{E}_{as}^\dagger(t_4) \hat{E}_{as}^\dagger(t_3) \hat{E}_s^\dagger(t_2) \hat{E}_s^\dagger(t_1) \hat{E}_s(t_1) \hat{E}_s(t_2) \hat{E}_{as}(t_3) \hat{E}_{as}(t_4) \rangle. \quad (3)$$

The normalized fourth-order cross-correlation is

$$g_{s,s,as,as}^{(4)}(t_1, t_2, t_3, t_4) = \frac{\langle \hat{E}_{as}^\dagger(t_4) \hat{E}_{as}^\dagger(t_3) \hat{E}_s^\dagger(t_2) \hat{E}_s^\dagger(t_1) \hat{E}_s(t_1) \hat{E}_s(t_2) \hat{E}_{as}(t_3) \hat{E}_{as}(t_4) \rangle}{\langle \hat{E}_s^\dagger(t_1) \hat{E}_s(t_1) \rangle \langle \hat{E}_s^\dagger(t_2) \hat{E}_s(t_2) \rangle \langle \hat{E}_{as}^\dagger(t_3) \hat{E}_{as}(t_3) \rangle \langle \hat{E}_{as}^\dagger(t_4) \hat{E}_{as}(t_4) \rangle}. \quad (4)$$

$G_{s,s,as,as}^{(4)}(t_1, t_2, t_3, t_4)$  can be expressed in terms of the first-order auto and cross-correlations between the modes as shown in Appendix ??.

We search for four-fold coincidences for detections at times  $t_1$  to  $t_4$  in channels 1 to 4, under the same conditions as in section ??, within a window of 100 ns. We represent the data as sliced density plots where each slice shows quadruplets for a fixed delay  $\tau_{12}$  and various relative delays  $\tau_{31}$  and  $\tau_{41}$ . We see the maximum density of quadruplets clustered around  $\tau_{12} = 0 \pm 2$  ns and  $\tau_{31}$  and  $\tau_{41} = 8 \pm 2$  ns. Outside a 20 ns window centered at  $(\tau_{12}, \tau_{31}, \tau_{41}) = (0 \text{ ns}, 8 \text{ ns}, 8 \text{ ns})$  the quadruplet count drops significantly to the background level indicating the presence of highly-correlated quadruplets within 20 ns. Every slice contains bright horizontal and vertical ridges from four-fold coincidences between accidentals and a correlated pair between Ch4-Ch1 or Ch3-Ch1 respectively. A relatively dull diagonal due to four-fold coincidences between accidentals and thermally bunched photons in Ch3-Ch4 can also be seen.

### D. Detection Rates

From the data we obtain singles rates in each channel ( $R_i, i \in \{1, 2, 3, 4\}$ ) and singles in the Stokes (anti-

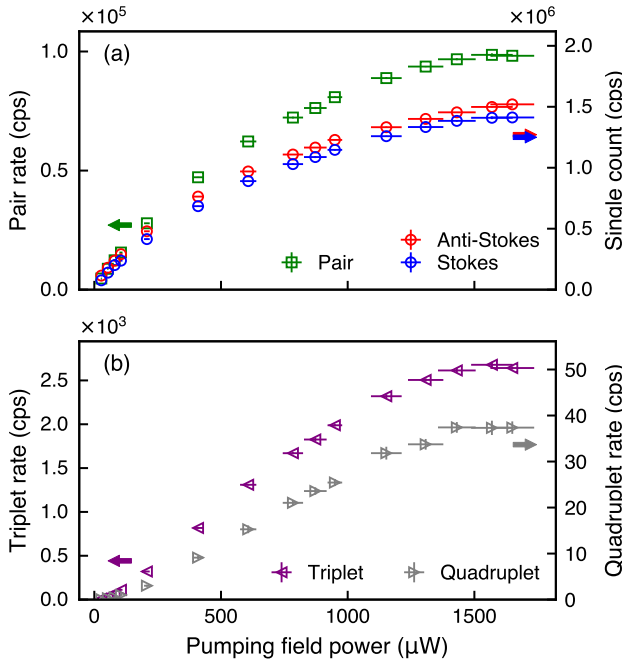


FIG. 5. Detection rates as a function of pump power (a) Single count rates (left axis) in Stokes (blue dots) and anti-Stokes channels (red dots) and correlated photon pair rate (green dots, right axis) as functions of pumping field power. (b) Correlated photon triplet rates across three detector channels (magenta dots, left axis) and correlated photon quadruplet rate (grey dots, right axis) as functions of pumping field power. The detuning of the pumping field is 40 MHz, while the coupling field is resonant with a fixed power of 10 mW. The atomic cloud has  $\text{OD} \simeq 30$ .

Stokes) modes as  $R_{s(as)} = R_{1(3)} + R_{2(4)}$ . From the pair, triplet and quadruplet coincidence measurements we obtain the measured pair rate as  $R_p = R_{13} + R_{14} + R_{23} + R_{24}$  ( $R_{ij}$  is the rate for coincidences between channels  $i$  and  $j$ ), triplet rate  $R_t = R_{134} + R_{234} + R_{123} + R_{124}$  ( $R_{ijk}$  is the rate for coincidences between channels  $i$ ,  $j$  and  $k$ ), and quadruplet rate ( $R_q$ ) defined within a  $t_c = 20$  ns coincidence window, without subtraction of accidentals.  $t_c$  of 20 ns is appropriate as the detection of correlated double-pairs is peaked within this window as seen from sections ?? and ???. Fig.?? shows the singles, pairs, triplets and quadruplet rates as functions of pump power. The photon pair and quadruplet production saturate at pump powers over a mW. At low pump powers (approximately  $< 200 \mu\text{W}$ ) the pair rate scales linearly with the pump power while the triplet and quadruplet rate scales quadratically with the pump power.

This is better visualized in Fig. ??, where the pair, triplet and quadruplet rates are shown relative to singles rates in the Stokes and anti-Stokes modes, with axes in log scale.  $R_p$  scales approximately linearly with  $R_s$  and  $R_{as}$ , with fitted slope parameters of  $0.86 \pm 0.02$  and  $0.95 \pm 0.03$ , respectively. The slopes of  $R_t$  and  $R_q$  relative to  $R_s$  are  $1.87 \pm 0.02$  and  $2.11 \pm 0.03$ , respectively, while

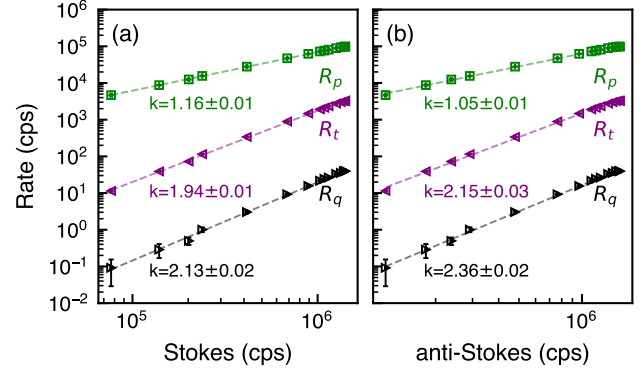


FIG. 6. Ratio of pairs, triplets and quadruplets to singles. The photon pair rate  $R_p$  (green dots), photon triplet rate  $R_t$  (magenta dots), and photon quadruplet rate  $R_q$  (black dots) from Fig. ?? represented in log-scale relative to the singles count rate  $R_s$  in Stokes mode (a) and singles count rate the anti-Stokes  $R_{as}$  (b). Both axes are plotted on a logarithmic scale. The variation in the single count rates is achieved by varying the pump power while keeping all other parameters constant.

the slopes of  $R_t$  and  $R_q$  relative to  $R_{as}$  are found to be  $1.97 \pm 0.04$  and  $2.34 \pm 0.03$ , respectively. The slopes of  $R_t$  and  $R_q$  are both close to 2 which is expected from the fact that triplet and quadruplet photons originate from the same physical processes. Furthermore, these measurements indicate that the rate at which double-pairs are detected scales close to quadratically with the rate of detecting correlated photon-pairs, which shows that the photons in the double-pairs are produced from a higher-order process in frequency conversion. However, to identify the exact relationship between the probability of generating states with four photons and states with pairs of photons, we need to correct for accidentals and factor losses from inefficient optical paths, photon collection and detection in each channel.

### E. Accidental corrected detection rates and generation rate

At fixed pump and coupling powers of  $800 \mu\text{W}$  and 10 mW respectively, and  $\Delta_p = 40$  MHz, the mean value of singles rates  $R_s$  is  $(1.04 \pm 0.07) \times 10^6$  cps and  $R_{as}$  is  $(1.10 \pm 0.06) \times 10^6$  cps. To determine the rates of truly correlated pairs, triplets and quadruplets from the detected pair, triplet, and quadruplet rates, we performed accidental correction as described in the Appendix ???. This gives a correlated pair detection rate  $c_p = (4.8 \pm 0.3) \times 10^4$  cps.

As we can see in Appendix ???, the correction of accidentals for triplets depends on which mode is used as the herald. Thus, we report channel-specific accidental-corrected triplet rates. The corrected rate of detected photon triplets consisting of one Stokes photon and two anti-Stokes photons in Ch3 and Ch4 is  $c_{134} + c_{234} =$

$(251 \pm 10)$  cps, while the rate for triplets consisting of two Stokes photons in Ch1 and Ch2 and one anti-Stokes photon is  $c_{123} + c_{124} = (246 \pm 7)$  cps. Here  $c_{ijk}$  is the rate of correlated triplets between channels  $i$ ,  $j$  and  $k$ . The correlated photon quadruplet rate after accidental-subtraction is found to be  $c_q = (2.9 \pm 0.4)$  cps. The total transmission and detection probability in each channel  $k \in \{1, 2, 3, 4\}$ , which includes transmission of the collection and filtering setup, splitting efficiency of the fiber-based 50:50 beamsplitter and quantum efficiency of the detector in the respective channel is denoted by  $\eta_k$ . Following the procedure in Appendix ?? to estimate the losses in each channel, we find the total efficiencies to be  $\eta_1 = 0.022$  and  $\eta_2 = 0.023$  for channels 1 and 2 pertaining to the Stokes modes, and  $\eta_3 = 0.025$  and  $\eta_4 = 0.021$  for channels 3 and 4 of the anti-Stokes mode.

We infer the generation rates of pairs  $g_p$  and double-pairs  $g_q$  from detected accidental-corrected rates of pairs, triplets and quadruplets by factoring in the channel losses as described in ???. Based on this, we report a double-pair generation rate of  $g_q = 2.5(4) \times 10^6$  cps and a pair generation rate of  $g_p = 1.3(3) \times 10^7$  cps at a pump power of  $800 \mu\text{W}$ .

#### IV. CONCLUSION

•

#### Appendix A: Double, Triple and Quadruple Coincidences

Here we express the double, triple and quadruple coincidence rates in terms of the phase sensitive first-order cross-correlation,

$$C(\tau_{ij}) = \langle \hat{E}_i(t + \tau_{ij}) \hat{E}_j(t) \rangle \quad (\text{A1})$$

and the first-order autocorrelation

$$R(\tau_{ij}) = \langle \hat{E}_i^\dagger(t + \tau_{ij}) \hat{E}_j(t) \rangle \quad (\text{A2})$$

where  $\{i, j\} \in \{s, as\}$  to represent the Stokes or anti-Stokes modes or  $\{i, j\} \in \{1, 2, 3, 4\}$  to represent one of the four detection channels. Note,  $R(0)$  is the pair generation rate.

It is well known that when the state under consideration is the output of a parametric photon-pair production such as SPDC or SFWM, the Gaussian moment factoring theorem can be applied to the intensity correlations in Eq.?? to give the following expression for the normalized intensity cross-correlation [?]

$$g_{s,as}^{(2)}(\tau) = 1 + \frac{|C(\tau_{s,as})|^2}{|R(0)|^2}, \quad (\text{A3})$$

and the normalized intensity autocorrelation as

$$g_{i,i}^{(2)}(\tau) = 1 + \frac{|R(\tau_{i,i})|^2}{|R(0)|^2} \quad (\text{A4})$$

The triple-coincidence rate  $G_{as,as,s}^{(3)}$  for two anti-Stokes detections and a single Stokes detection,

$$G_{as,as,s}^{(3)}(t_3, t_4, t_s) = \langle \hat{E}_s^\dagger(t_s) \hat{E}_{as}^\dagger(t_3) \hat{E}_{as}^\dagger(t_4) \hat{E}_{as}(t_4) \hat{E}_{as}(t_3) \hat{E}_s(t_s) \rangle \quad (\text{A5})$$

can be similarly expanded and expressed in terms of relative delays to give [? ?]

$$\begin{aligned} G_{as,as,s}^{(3)}(\tau_{3s}, \tau_{4s}, \tau_{34}) &= R(0)[R(0)^2 + |R(\tau_{34})|^2] \\ &\quad + R(0)[|C(\tau_{3s})|^2 + |C(\tau_{4s})|^2] \\ &\quad + 2\text{Re}\{C(\tau_{3s})C^*(\tau_{4s})R(\tau_{34})\}. \\ &= R(0)^3 g_{as,as}^{(2)}(\tau_{34}) + R(0)^3 g_{as,s}^{(2)}(\tau_{3s}) \\ &\quad + R(0)^3 g_{as,s}^{(2)}(\tau_{4s}) - 2R(0)^3 \\ &\quad + 2R(0)^3 \sqrt{g_{as,s}^{(2)}(\tau_{3s}) - 1} \\ &\quad \times \sqrt{g_{as,s}^{(2)}(\tau_{4s}) - 1} \times \sqrt{g_{as,as}^{(2)}(\tau_{34}) - 1}. \end{aligned} \quad (\text{A6})$$

This equation shows that accidental triplet events are a sum of four contributions: accidental singles detected in each of the three channels, a correlated pair between the Stokes mode and Ch3 (Ch4) with an accidental in Ch4 (Ch3) and thermally bunched photons in the anti-Stokes (causing coincidences in Ch3 and Ch4) with an accidental single in the Stokes mode (Ch1 or Ch2). The normalized third-order correlation can be expressed in terms of the normalized intensity auto and cross correlations using ?? and ?? as

$$\begin{aligned} g_{as,as,s}^{(3)}(\tau_{3s}, \tau_{4s}, \tau_{34}) &= \frac{G_{as,as,s}^{(3)}(\tau_{3s}, \tau_{4s}, \tau_{34})}{R(0)^3} \\ &= g_{as,as}^{(2)}(\tau_{34}) + g_{as,s}^{(2)}(\tau_{3s}) \\ &\quad + g_{as,s}^{(2)}(\tau_{4s}) - 2 \\ &\quad + 2\sqrt{g_{as,s}^{(2)}(\tau_{3s}) - 1} \sqrt{g_{as,s}^{(2)}(\tau_{4s}) - 1} \\ &\quad \times \sqrt{g_{as,as}^{(2)}(\tau_{34}) - 1}. \end{aligned} \quad (\text{A7})$$

Similarly, the quadruplet rate for detecting two Stokes photons at times  $t_1$  and  $t_2$  and two anti-Stokes photons at times  $t_3$  and  $t_4$  is given in Eq.??, where the moment factoring theorem was applied to obtain the following

expression in terms of relative delays.

$$\begin{aligned}
G_{s,s,as,as}^{(4)}(\tau_{34}, \tau_{24}, \tau_{14}, \tau_{23}, \tau_{21}, \tau_{13}) = & R(0)^4 \\
& + R(0)^2[|R(\tau_{43})|^2 + |R(\tau_{21})|^2] \\
& + R(0)^2[|C(\tau_{23})|^2 + |C(\tau_{24})|^2] \\
& + R(0)^2[|C(\tau_{13})|^2 + |C(\tau_{14})|^2] \\
& + 2R(0)\text{Re}\{R(\tau_{34})C^*(\tau_{24})C(\tau_{23})\} \\
& + 2R(0)\text{Re}\{R(\tau_{34})C^*(\tau_{14})C(\tau_{13})\} \\
& + 2R(0)\text{Re}\{R(\tau_{21})C^*(\tau_{14})C(\tau_{24})\} \\
& + 2R(0)\text{Re}\{R(\tau_{21})C^*(\tau_{13})C(\tau_{23})\} \\
& + |R(\tau_{43})|^2|R(\tau_{21})|^2 \\
& + |C(\tau_{13})|^2|C(\tau_{24})|^2 + |C(\tau_{14})|^2|C(\tau_{23})|^2 \\
& + 2\text{Re}\{C^*(\tau_{24})C^*(\tau_{13})C(\tau_{14})C(\tau_{23})\} \\
& + 2\text{Re}\{R(\tau_{34})R(\tau_{12})C^*(\tau_{24})C(\tau_{13})\} \\
& + 2\text{Re}\{R(\tau_{34})R(\tau_{21})C(\tau_{23})C^*(\tau_{14})\}
\end{aligned} \tag{A8}$$

From the 17 terms that sum up to give  $Q$  in Eq ??, all terms other than the last three are contributions due to accidentals. Terms 2-7, are due to two accidentals combined with either a correlated Stokes-anti-Stokes pair or bunched photons in one of the Stokes or anti-Stokes modes. Terms 8-11 are caused by an accidental combined with a correlated triplet in three channels. Term 12 is from bunching in both the Stokes and anti-Stokes modes. Terms 13 and 14 are correlated pairs from separate SFWM events contributing to four-fold coincidences. Terms 15, 16 and 17 are due to correlated double-pairs from the same SFWM event.

## Appendix B: Event searching algorithms

The search for multiple coincidences over timestamp data of four channels is a computationally resource intensive task. We employ the following strategy to simplify the search. We first identify pair coincidences at various relative delays for each pair from the following possible pairs of Stokes-anti-Stokes channels 1-3, 1-4, 2-3 and 2-4. The triplet coincidences are then identified based on the pair detections that share a photon arrival timestamp. Quadruplet events are identified from triplet detections that share a common timestamp with a pair detection.

For example, to identify triplet events involving Ch1, Ch3, and Ch4, we compare the timestamps of pairs between Ch1 and Ch3 detected at timestamps  $t_1$  and  $t_3$  with pairs between Ch1 and Ch4 detected at timestamps  $t'_1$  and  $t_4$ . Pair events that share a common timestamp in Ch1 i.e.  $t_1 = t'_1$ , are taken to form the triplet event  $(t_1, t_3, t_4)$ . This information can be used to identify quadruplets between the four channels. For this we compare pair events between Ch2 (at  $t_2$ ) and Ch4 (at time  $t_4^*$ ) with the previously identified triplet event with times  $t_1, t_3, t_4$ . When  $t_4 = t_4^*$ , the events are combined to form a quadruplet detection with the times-

tamp  $t_1, t_2, t_3, t_4$ . Thus, we can efficiently search for pair, triplet, and quadruplet events from timestamp data and plot the temporal distribution of these coincidences.

## Appendix C: Channel Losses

We characterize the losses in each channel to estimate the rate of correlated pairs and double-pairs directly generated from the SFWM process. The total transmission and detection probability in each channel  $k \in \{1, 2, 3, 4\}$ , which includes transmission of the collection and filtering setup, splitting efficiency of the fiber based 50:50 beam-splitter and quantum efficiency of the detector in the respective channel is denoted by  $\eta_k$ . The optical losses in each channel are determined by measuring the transmission of a laser beam (at the target wavelength) from outside the vacuum chamber to just before the detector in each channel. We measure transmissions of  $\approx 11.5\%$  each for Ch1 and Ch2 and  $12.5\%$  each for Ch3 and Ch4, which include the contributions from the filter-Etalon and fiber beamsplitter. Including the quantum efficiencies of APDs in each channel (about 60-70% per APD), the measured efficiencies ( $\eta'_k$ ) for each channel are 0.078, 0.083, 0.080, and 0.067 for channels 1,2,3 and 4 respectively. These values provide an estimate of the upper bound for effective efficiencies, as they do not account for absorption in the atomic ensemble or spatial mode mismatch between the photons and the collection optics.

Since we expect additional losses that are frequency specific to the Stokes and anti-Stokes modes, we define  $\eta_i = \eta_s \eta'_i$  for  $i \in \{1, 2\}$  and  $\eta_j = \eta_{as} \eta'_j$  for  $j \in \{3, 4\}$ . We then use equations ?? and ?? to estimate  $\eta_s$  and  $\eta_{as}$ . We infer additional losses that are  $1 - \eta_s = 19\%$  for channels in the Stokes arm and  $1 - \eta_{as} = 8\%$  for the anti-Stokes channels, which we attribute to a combination of above mentioned factors. Taking into account these additional losses, the total efficiencies are  $\eta_1 = 0.022$  and  $\eta_2 = 0.023$  for channels 1 and 2 pertaining to the Stokes modes, and the total efficiencies are  $\eta_3 = 0.025$  and  $\eta_4 = 0.021$  for channels 3 and 4 of the anti-Stokes mode.

## Appendix D: Generation Rates from Detection Rates

We infer the generation rates of pairs  $g_p$  and double-pairs  $g_q$  from the detected accidental-corrected rates of pairs, triplets and quadruplets by factoring in the channel losses as follows.  $c_q$ , the accidental-corrected quadruplet rate, is solely contributed to by generated double-pairs as well. There are four possible combinations by which the two Stokes photons reach Ch1 and Ch2 each and the two anti-Stokes photons reach Ch3 and Ch4 each. This gives,

$$c_q = 4g_q \eta_1 \eta_2 \eta_3 \eta_4. \tag{D1}$$

Similarly, double-pair generations are the sole contributors to accidental-corrected triplet coincidences. A triplet between channels 1, 3 and 4 occurs from two possible combinations by which the two anti-Stokes photons reach one of Ch3 and Ch4 each (leading to the factor  $2\eta_3\eta_4$ ) combined with the probability that at least one of the two Stokes photons reaches Ch1 (leading to the factor  $1 - (1 - \eta_1)^2$  where  $(1 - \eta_1)^2$  is the probability that neither of the two Stokes photons reaches channel 1). Applying this to all combinations of triplet detections,

$$\begin{aligned} c_{123} &= 2g_q\eta_1\eta_2(2 - \eta_3)\eta_3 \\ c_{124} &= 2g_q\eta_1\eta_2(2 - \eta_4)\eta_4 \\ c_{134} &= 2g_q\eta_3\eta_4(2 - \eta_1)\eta_1 \\ c_{234} &= 2g_q\eta_3\eta_4(2 - \eta_2)\eta_2. \end{aligned} \quad (\text{D2})$$

We use this to estimate mean values of  $g_q$ . Since we have non-number-resolving detectors, both pairs and double-pairs from the SFWM process contribute to pair coincidence detections. A coincidence between channels 1 and 3 can be caused by a generated pair where the Stokes photon is detected in Ch1 and the anti-Stokes is detected in Ch3 ( $\eta_1\eta_3$ ) or the probability that at least one of two Stokes and two anti-Stokes photons from a double-pair reach Ch1 and Ch3 respectively  $((1 - (1 - \eta_1)^2)(1 - (1 - \eta_3)^2) = \eta_1\eta_3(2 - \eta_1)(2 - \eta_3))$ . This gives,

$$\begin{aligned} c_{13} &= \eta_1\eta_3(g_p + g_q(2 - \eta_1)(2 - \eta_3)) \\ c_{14} &= \eta_1\eta_4(g_p + g_q(2 - \eta_1)(2 - \eta_4)) \\ c_{23} &= \eta_2\eta_3(g_p + g_q(2 - \eta_2)(2 - \eta_3)) \\ c_{24} &= \eta_2\eta_4(g_p + g_q(2 - \eta_2)(2 - \eta_4)) \end{aligned} \quad (\text{D3})$$

where  $c_{ij}$  is the accidental-corrected pair rate between channels  $i$  and  $j$ .

We use measured accidental-corrected pair, triplet and quadruplet rates to obtain values for  $g_p$  and  $g_q$ , and the mean values are reported in section ??.

## Appendix E: Accidental Correction Procedure

Correction must be performed to eliminate contributions from accidental coincidences between uncorrelated events from different channels. This can be visualized as the relative probability of two independent events falling within the same coincidence time window  $t_c$  (i.e. random chance), yielding the accidental rate  $t_c R_i R_j$  for singles rates  $R_i$  and  $R_j$  in channels  $i$  and  $j$ . Excess coincidence events after correction can then only be attributed to actual correlations between channels: in the case of two

channels  $i$  and  $j$  with an observed pair rate of  $R_{ij}$ , the correlated pair rate  $c_{12}$  is given by

$$c_{ij} = R_{ij} - t_c R_i R_j.$$

The total correlated pair rate is  $c_p = \sum_{i,j} c_{ij}$  for  $\{i, j\} \in \{\{1, 3\}, \{1, 4\}, \{2, 3\}, \{2, 4\}\}$ .

These correlated pairs (and separately, accidentals) can be modeled as a separate stream of events that factor into the calculation of higher-order accidentals, e.g. 3-fold accidentals between channels  $i, j$  and  $k$  occur due to accidental coincidences across the individual channels  $\{R_i, R_j, R_k\}$ , as well as pairs with the remaining channel  $\{c_{ij}, R_k\}$ ,  $\{c_{ik}, R_j\}$  and  $\{c_{jk}, R_i\}$ . For instance, in Fig. ?? these correspond to the general background horizontal, vertical ridges and diagonal ridges when  $\{i, j, k\} = \{s, 3, 4\}$ .

The correlated triplet rate is thus

$$c_{ijk} = R_{ijk} - t_c (c_{ij}R_k + c_{jk}R_i + c_{ik}R_j) - t_c^2 R_i R_j R_k$$

given an observed triplet rate of  $R_{ijk}$ .

It can be seen that each of the individual terms contributing to the  $n$ -fold coincidences correspond to a possible partitioning of the set of all channels, with the total number of partitions given by Bell's number  $B_n$  (i.e.  $B_2 = 2$ ,  $B_3 = 5$ ,  $B_4 = 15$ ). We write out explicitly the exhaustive 14-term correction performed for 4-fold coincidences,

$$\begin{aligned} c_{1234} &= R_{1234} \\ &- t_c (c_{12}c_{34} + c_{13}c_{24} + c_{14}c_{23}) \\ &- t_c (c_{123}R_4 + c_{124}R_3 + c_{134}R_2 + c_{234}R_1) \\ &- t_c^2 (c_{12}R_3R_4 + c_{13}R_2R_4 + c_{14}R_2R_3) \\ &- t_c^2 (c_{23}R_1R_4 + c_{24}R_1R_3 + c_{34}R_1R_2) \\ &- t_c^3 R_1R_2R_3R_4. \end{aligned}$$

We also make a small note that this correction slightly overestimates the actual accidental rate [?] due to the  $n$ -fold coincidence calculation method containing an implicit ordering of events that introduces excess accidentals. This overcompensation is minimized by using a small 20 ns coincidence window, yielding a raw quadruplet rate of 20.5 cps and lower bound correlated quadruplet rate of 3 cps with the experimental settings... Most of the accidentals are dominated by pair-pair accidentals (5.5 cps), followed by pair-acc-acc (5.6 cps) and triplet-acc (4.8 cps). **These numbers need to be updated based on actual calculations**

Code for the accidental correction as well as the corresponding datasets can be found in...